Customer	**:**	**ESA/ESRIN**	**Document Ref**	**:**	**CALIB-TN-WP230-SES-VEGA**
Contract No	**:**	**21125/07/1-OL**	**Issue Date**	**:**	**12 novembre 2008**
WP No	**:**	**230**	**Issue**	**:**	**001**

Title : **Calibration Test Sites Selection and Characterisation**
WP 230 - The Sea Equipped Sites

Abstract : This document describes the geophysical properties relevant to vicarious calibration.

Author : Richard SANTER;

Approval B. Berthelot

Accepted P. Goryl

Distribution : **Hard Copy File:**
Filename: CALIB-TN-WP230-SES-VEGA_001.doc

VEGA Technologies SAS
12, Avenue de l'Europe, Villa San Diégo, Parc technologique du canal, 31520 Ramonville Saint Agne, France
Tel: +33 (0)5.67.77.19.99 Fax: +33 (0)5.67.77.19.98
www.vega-group.com

This Page Is Intentionally Blank

TABLE OF CONTENTS

LIST OF FIGURES

LIST OF TABLES

REFERENCES AND APPLICABLE DOCUMENTS

RD.1 CEOS reports,http://wgcv.ceos.org/documentation/wgcv24.htm

RD.2 Cal/Val portal, 2nd MERIS AATSR validation Team meeting, http://envisat.esa.int/workshops/mavt_2006/MAVT-2006-0104_CBrockmann.pdf

RD.3 SPPA functional baseline, ESA Document Reference,PGSI-EOPG-TN-05-0025, http://emits.esa.int/emits-doc/ESRIN/1-5300/SPPA_GS_requirements_v1.2.pdf

RD.4 Spot 5 in-flight commissioning: inner orientation of HRG and HRS instruments, R.Gachet, CNES/IGN,http://www.isprs.org/HRS/PDF/96.pdf

RD.5 Post-Launch Calibration Of Satellite Sensors, ISPRS Book Series – Volume 2,

RD.6 Status Of Meris validation Activities at BOUSSOLE site, 2nd MERIS AATSR Validation Team Meeting ,http://envisat.esa.int/workshops/mavt_2006/MAVT-2006-0802_DAntoine.pdf

RD.7 Basic Strategy for the Post-Launch calibration and characterization of Visible and Near-Infrared meteorological satellite sensors, C.R. Nagaraja Rao http://wgcv.ceos.org/docs/wgcv/post_launch_strategy.pdf

RD.8 Sentinel 2 Mission Requirement Document http://esamultimedia.esa.int/docs/GMES/MRD_Sentinel_2.pdf

RD.9 MERIS AATSR Validation Team workshop proceeding, 2006 http://envisat.esa.int/workshops/mavt_2006/

RD.10 The Simbios Program ,http://www.ioccg.org/reports/simbios/simbios.html

RD.11 Radiometric Calibration of IKONOS. using Ground-Reference Test. Sites, K. Thome http://ldcm.nasa.gov/library/HSRCIW02/Ground_Ref_Test_SitesThome.pdf

RD.12 Inflight intersensor radiometric calibration using vicarious approaches, K. Thome http://www.commission1.isprs.org/isprs_ceos_workshop/Documents/Thome/Thome.pdf

RD.13 MERIS AATSR Validation Team workshop proceeding, 2006 http://envisat.esa.int/workshops/mavt_2006/

RD.14 Study of Natural Calibration Sites for the Cloud Profiling Radar Final Report ESA Contract 16474/02/NL, May 2005.

RD.15 Joint ISPRS/CEOS-WGCV Task Force on Radiometric and Geometric Calibration, S.A. Morain, V.M. Zanoni Commission I, WG I/2.

RD.16 D1-3: Calibration Requirements Consolidation, Deliverable from the EO calval project.

RD.17 Mazeran C., 2007. Quality Control methodology for validating Ocean Atmospheric Correction, Report, ACRI ST.

RD.18 Berthelot, B and R. Santer, Adequacy of the selected sites with respect to the atmospheric/surface parameters, CALIB-TN-WP230-VEGA_001.pdf.

RD.19 Berthelot B. R. Santer, S. Saunier, P. Blanc, 2008, Sensors list/classification according to the need for vicarious classification, document VEGA, CALIB-TN-WP110-VEGA-001.

AD.1 Calibration Test Sites Selection and Characterisation, Issue 1.7 dated 02/03/2007, GMES-CLVL-EOPG-SW-06-0004

AD.2 Project Management Plan, VEGA-CTSS-070197-PMP_1.0

GLOSSARY

The Glossary contains definitions of acronyms, abbreviations and terms used throughout the document.

AAOT	Acqua Alta Oceanographic Tower
BOUSSOLE	BOUée pour l'acquiSition de Séries Optiques à Long termE
BRDF	Bi-directional Reflectance Distribution Function
BRF	Bi-directional Reflectance Function
Cal/Val	Calibration and Validation
CEOS	Committee on Earth Observation Satellites
ENVISAT	ENVIronment SATellite
EO	Earth Observation
ESA	European Space Agency
ITT	Invitation To Tender
IVOS	Infrared and Visible Optical Sensors
LES	Land Equipped Site
LNES	Land Non Equipped Site
MAVT	MERIS & AATSR Validation Team
MERIS	Medium Resolution Imaging Spectrometer
MOBY	Marine Optical Buoy
PMP	Project Management Plan
RMS	Root Mean Square
RT	Radiative Transfer
RTC	Radiative Transfer Code
Sentinel	Family of ESA spacecrafts
SES	Sea Equipped Site
SNES	Sea Non Equipped Site
SOW	Statement Of Work
TBC	To Be Confirmed
TBD	To be Defined
TOA	Top Of Atmosphere
VIS	Visible
VOS	Visible Optical Sensors
WGCV	Working Group on Calibration and Validation
WP	Work Package

AMENDMENT POLICY

This document shall be amended by releasing a new edition of the document in its entirety. The Amendment Record Sheet below records the history and issue status of this document.

AMENDMENT RECORD SHEET

ISSUE	DATE	DCI No	REASON
A	20 Nov 2008	N/A	Initial Issue
B			

1. INTRODUCTION

1.1 Overview of the project: purpose and scope

This study is part of the ESA strategy for ensuring the quality (calibration, validation and operational quality) of data developed for current and future missions within the Explorers and GMES framework.

The scope of the project is to select, identify and characterise reference test sites that will be used for the calibration and characterisation of different sensor types. The characteristics of the sites that will be provided at the end of this study will be incorporated in the Cal/Val portal.

The project is composed of four tasks.

- The first task (WP100) aims at identifying the needs per sensors in terms of external (vicarious) calibration.
- The second task (WP200) aims at identifying and, characterising remote test sites that can be used for external calibration according to the needs previously described in WP 100.
- The third task (WP300) will perform the synthesis adapted to Sentinels satellites. The output of this task will help ESA in the definition of the strategy for external calibration of Sentinel instruments.
- The fourth task aims at giving ESA the support for the integration of identified sites into the ESA Cal/Val portal.

WP 100 is achieved and documented in RD.19. This document is a part of WP 200.

1.2 Objectives of the WP 200: “Identification and characterisation of remote test sites”

WP 200 aims at identifying and characterising the reference test sites used for vicarious calibration of sensors belonging to the sensor class 2 or 3[1], which are defined in RD.19.

For this, several steps are chaining in order to affine the characterisation, then the choice of reference test sites.

- In WP 210, the reference test sites used for vicarious calibration have been identified, and classified based on their intrinsic properties.
- WP 220 reviews the calibration methods used and identifies the appropriate sites, respectively for the radiometric (WP 221), geometric (WP 222), spectral (WP 223) and image quality (WP 224) aspects.
- WP 230 assesses the adequacy of the choice criteria of the sites in order to identify sites that minimize the source of errors in the calibration process.
- The objective of WP 240 is to collect information about available site equipment and required auxiliary data to lead correct calibration processes.
- WP 250 objective is to study the interest of grouping some sites presenting same characteristics in order to answer to technical requirements, limit efforts of coordination or ensure homogenised maintenance …

[1] *Class 2 is low spatial resolution sensors, class 3 is high spatial resolution sensors.*

- An error budget for four calibration sites is made in WP 260, accounting for surface and parameters.

Output of WP 200 will be used in WP 300 in order to define a strategy for vicarious calibration of the Sentinel mission (Figure 1).

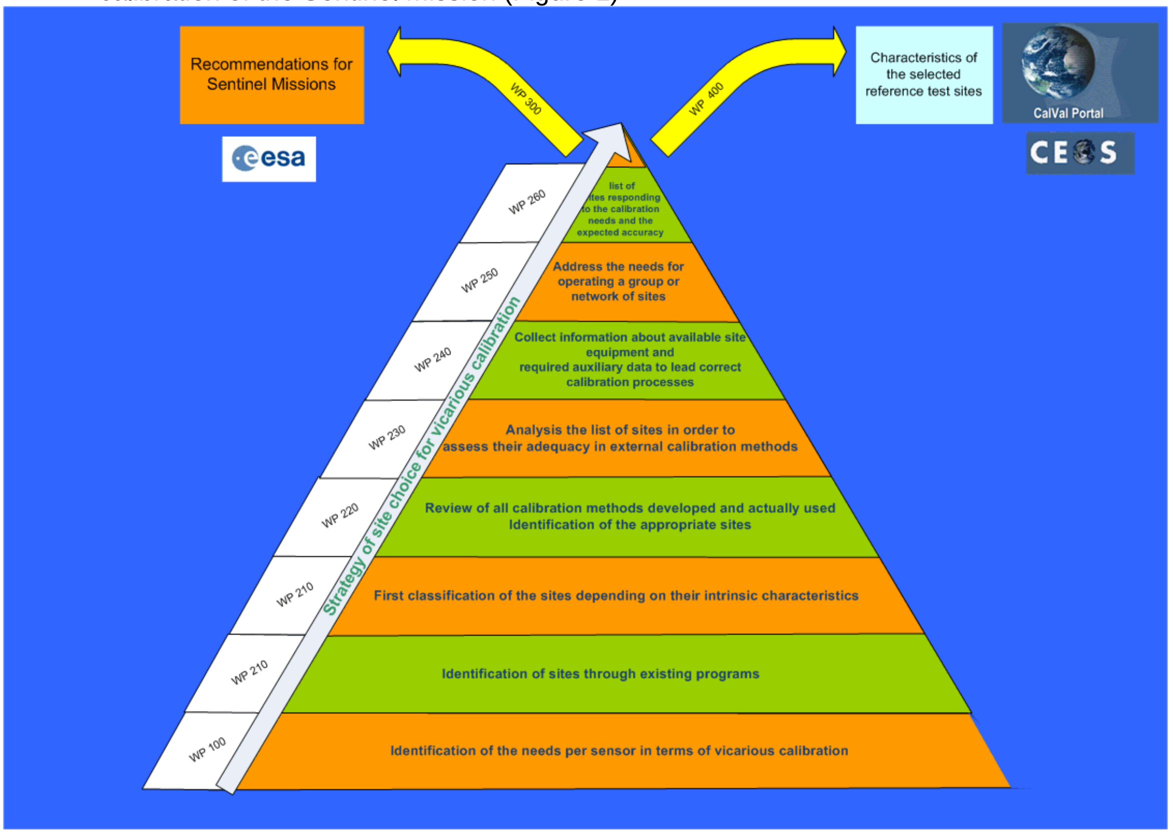

Figure 1: WP 200 activities for defining the vicarious calibration strategy used for S2/S3 sensors.

1.3 Objectives of the WP 230: Analysis of the sites in order to assess their adequacy in external calibration methods

The objectives of the Work Package are to analyse the sites previously identified in order to assess their adequacy in external calibration methods. This document focuses on Sea Equipped Site analysis.

2. SEA EQUIPPED SITE EVALUATION

The evaluation of the SES is conducted on:

- AERONET for the aerosols
- The MERIS Data Quality Working Group data base. This data base was built by ACRI under ESA contract (Mazeran, 2007) using the *in situ* data collected in Venice (PI: G. Zibordi), on BOUSSOLE (PI: D. Antoine) and on MOBY (PI:M. Ondrusek).

2.1 The water reflectance

The mean normalized (sun at zenith, nadir view) reflectances of the water and the associated r.m.s. are reported in Table 1, Table 2, and Table 3 for the 3 sites.

Table 1: Above water reflectance at MOBY: 142 datasets were used.

MOBY	412	443	490	510	560	620	665	681	708
mean	3.71E-02	2.86E-02	1.88E-02	1.01E-02	3.96E-03	3.72E-04	1.28E-04	1.21E-04	2.46E-05
sigma	5.14E-03	3.32E-03	1.65E-03	8.43E-04	4.01E-04	5.83E-05	2.13E-05	2.08E-05	4.43E-06

Table 2: above water reflectance at BOUSSOLE: 268 datasets were used.

BOUSSOLE	443	490	510	560	665	681
mean	1.45E-02	1.31E-02	9.38E-03	5.21E-03	4.60E-02	8.53E-02
sigma	4.26E-03	2.79E-03	1.61E-03	1.01E-03	3.35E-01	4.65E-01

Table 3: above water reflectance at AAOT: 114 datasets were used.

AAOT	412	443	490	560
mean	1.37E-02	1.62E-02	2.21E-02	1.78E-02
sigma	5.18E-03	6.46E-03	8.78E-03	8.80E-03

The reflectance of the three sites corresponds to what it is expected from clear water (MOBY) to more turbid water (AAOT) through the intermediate case of BOUSSOLE.

The stability of the water reflectance in MOBY may render possible to apply the so-called Rayleigh calibration in the blue.

2.2 The aerosols

For the closest AERONET station, we already indicated in RD.18 the climatology of the AOTs and their spectral dependence. BOUSSOLE is deserved by the too long distance from the coast line. Therefore any calibration method which relies on information on the aerosols will be not relevant for BOUSSOLE.

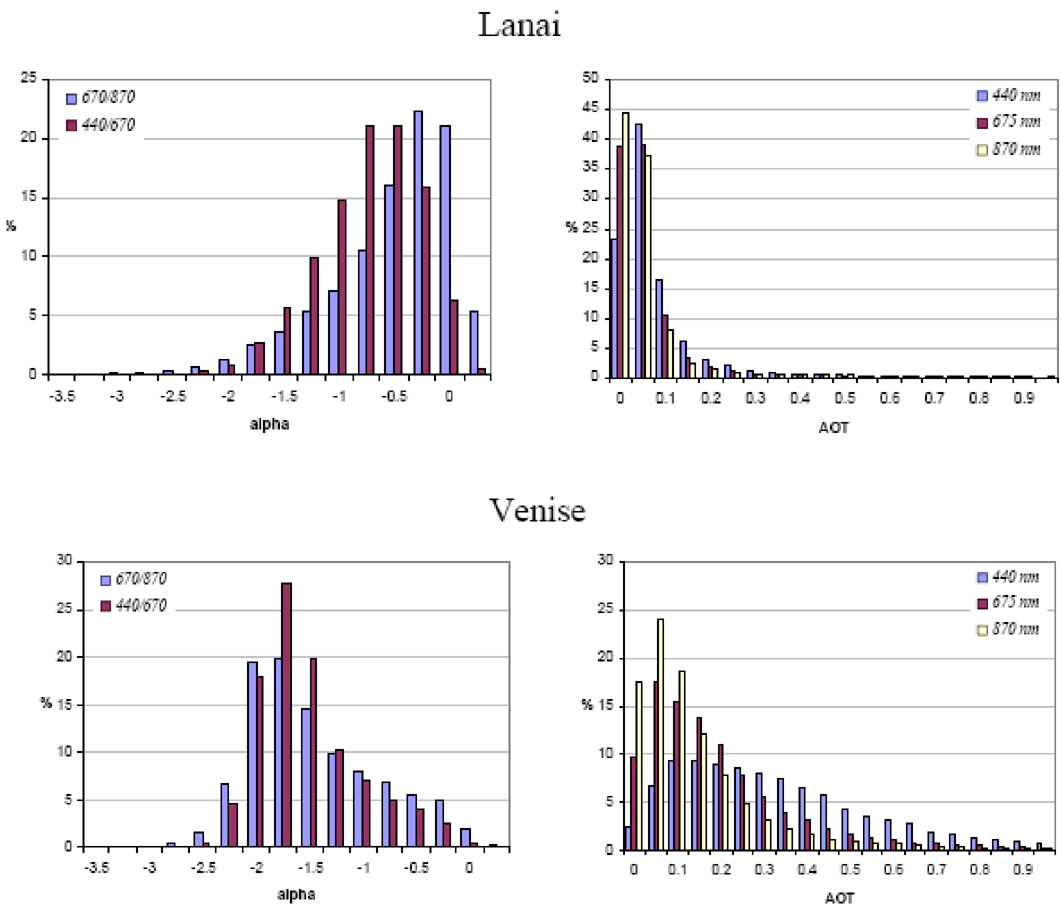

Figure 2: Histogram of the Angstroem coefficient (between 670-870 nm and 440-670 nm) and of the AOT as collected by AERONET in Lanai (MOBY) and in the AAOT.

Figure 2 indicates than a high probability of high visibility exists in MOBY with a quite narrow spectrum of Angstroem coefficient. Therefore, it seems to be easier to conduct vicarious calibration in MOBY compared to AAOT. This appreciation is temperate when we consider the MERIS aerosol level 2 products: AOT_865 and α as reported in Table 4.

Table 4: Two first lines: mean AOT at 865 nm and corresponding rms for the MERIS level 2 over the 3 sites. Two last lines: mean α at 865 nm and corresponding rms.

site	AAOT	MOBY	BOUSSOLE
AOT	0.171	0.078	0.116
dAOT	0.128	0.039	0.082
alpha	-1.01	-0.77	-0.77
dalpha	0.43	0.36	0.37

One other aspect to consider with the aerosols is the geometry. It is well known that the aerosol phase function increases in the backward scattering and is very sensitive to the aerosol model. The high occurrence of the backscattering geometry is a handicap for a calibration site. Table 5 clearly indicates that MOBY (or sites at this latitude) presents geometrical observations (for polar satellites with no sensor tilt) which are not favourable.

Table 5: Mean scattering angle Θ for the MERIS observations over the three sites. Percent of Θ>150°.

	AAOT	MOBY	Boussole
mean	129.3	153.4	132.3
<150°	77.1	35.9	74.1

2.3 Spatial homogeneity

We first use the MERIS flags to select data without any of the following flags raise.

LAND	CLOUD	ICE_HAZE	HIGH_GLINT	MEDIUM_GL	PCD_1_13	PCD_19	OADB	CASE2_S

2.3.1 Over MOBY

We extracted for MOBY, as reported in Table 6, the date, the number of selected pixels in the 5*5 RR pixel window, the average of AOT_865 and the relative dispersion of the TOA reflectance at 443 nm, 665 nm and 865 nm as the percent ratio of the rms by the mean. We also use the O_2 transmittance (TO_2) as the ratio of the TOA signal between 761 nm and 753 nm as well as the water vapour transmittance (ratio 900nm/885nm).

We can believe a priori that if we have few pixels then the dispersion of the signal within the window is higher because the flags suggest a high meteorological instability. Figure 3 follows this idea which is exceptionally relevant with two pixels. The heterogeneity has a strong origin the variation of the aerosols mainly as expected in B13 because of the decrease of the Rayleigh scattering. The dispersion does not increase with the AOT as illustrated by Figure 4. We can have turbid days with a strong spatial homogeneity in the NIR.

What is more relevant is to associate the heterogeneity of the aerosols with the O_2 transmittance as shown in Figure 5 with a clear correlation between the dispersion observed in B13 and the O_2 transmittance. In Figure 6 (corresponding to June 18, 2002), the transmittance decreases when B13 increases (more aerosols). The physical interpretation is the following: the O_2 transmittance is correlated to the altitude of the scatters, the molecules are higher than the aerosols. With no aerosols, you have a high O_2 transmittance corresponding to the molecules. If we increase the aerosol loading, the O_2 transmittance decreases because of to indicate than in mean the signal originates from the lower atmospheric layer. The process will be the reverse in the case of a contamination by the cirrus layer: TO_2 should increases with the signal in B13. The use of 761/753 is a key element of the quality control.

Table 6: spatial dispersion of MERIS TOA signal in MOBY (see text)

date	#	AOT	443	665	885	O2	TH2O
20020530	20	0.052	0.7	3.7	9.7	1.4	1.7
20020612	25	0.076	0.2	0.3	0.6	0.5	0.6
20020615	10	0.073	0.7	2.7	6.9	1.4	1.4
20020618	20	0.106	1.7	10.6	23.0	2.2	2.6
20020707	18	0.153	2.1	10.1	18.3	2.6	2.9
20020720	24	0.053	0.4	1.1	2.5	0.7	0.8
20020723	18	0.128	0.9	3.7	8.4	0.6	0.8
20020827	25	0.100	0.2	1.1	2.3	0.6	0.9
20020912	22	0.059	0.2	0.8	1.7	0.9	0.7
20020928	25	0.049	0.2	0.2	0.8	0.5	1.0
20021001	19	0.168	1.1	4.9	8.5	1.0	0.8
20021020	25	0.048	0.3	0.7	1.9	0.7	1.6
20021030	10	0.029	0.1	0.3	0.5	0.8	1.2
20021121	25	0.033	0.2	0.3	1.3	0.8	1.1
20021127	17	0.097	0.5	0.7	1.4	0.7	0.8
20021204	7	0.030	0.1	0.1	0.9	0.1	0.2
20021210	19	0.084	0.2	0.7	1.6	0.5	0.6
20021213	19	0.050	0.2	0.6	1.5	1.1	1.3
20021226	22	0.027	0.2	0.6	1.7	0.9	1.3
20030212	13	0.070	0.2	0.6	1.2	0.4	0.5
20030426	25	0.092	0.2	0.3	0.7	0.4	0.6
20030429	25	0.060	0.3	0.2	0.8	0.7	0.7
20030512	25	0.060	0.4	0.6	1.1	0.6	1.2
20030515	20	0.289	1.7	3.9	4.0	2.2	0.5
20030721	9	0.227	1.8	8.6	16.2	2.1	0.4
20030809	25	0.098	0.3	0.8	1.5	0.7	0.6
20030812	25	0.163	0.6	3.9	8.0	1.3	0.9
20030828	25	0.028	0.2	0.4	1.0	0.9	1.1
20030916	23	0.092	0.3	1.2	2.8	1.2	1.4
20030929	25	0.054	0.6	1.1	1.8	0.9	0.7
20031005	9	0.069	0.1	0.6	1.5	0.8	1.0
20031015	18	0.064	0.4	0.7	1.2	0.7	0.8
20031021	14	0.021	0.3	0.4	1.5	0.9	1.4
20031024	15	0.071	0.3	1.0	2.0	1.1	1.7
20031106	25	0.064	0.4	2.4	5.5	1.0	1.1
20031122	25	0.049	0.5	2.3	4.8	1.6	0.9
20031128	15	0.031	0.3	1.6	4.6	1.2	2.3
20031211	16	0.097	0.5	1.9	3.8	1.3	0.9
20040105	5	0.113	0.2	1.5	2.9	1.1	1.0
20040131	5	0.045	0.2	0.7	2.3	0.7	1.1
20040203	16	0.077	0.2	1.0	2.3	1.1	0.8
20040219	21	0.074	0.4	0.6	1.1	0.9	0.6
20040222	21	0.062	0.8	3.8	8.2	1.9	1.0
20040312	25	0.054	0.2	0.2	0.8	0.9	0.9
20040312	4	0.067	0.1	0.2	0.2	0.4	0.5
20040518	8	0.082	0.3	0.2	0.4	0.8	0.5
20040705	18	0.062	0.3	0.7	0.9	0.9	0.7
20040708	25	0.063	0.2	0.7	1.4	0.9	0.9
20040711	25	0.091	2.1	10.1	20.2	3.2	2.1
20040721	15	0.034	0.2	0.3	0.9	0.4	0.8
20040724	22	0.068	0.7	4.0	9.8	1.3	0.8
20040727	25	0.039	0.5	3.2	7.8	2.4	1.7
20040831	24	0.057	1.3	5.8	15.4	1.6	1.9

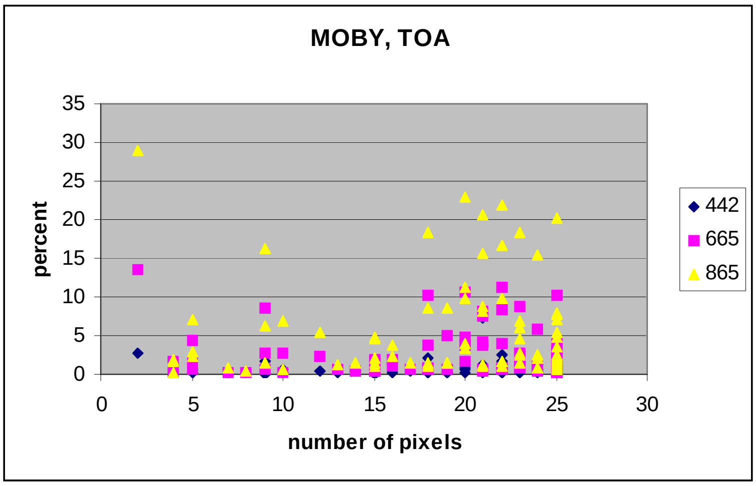

Figure 3: Relative dispersion of the MERIS TOA signal for the MOBY window depending on the number of pixels in the window.

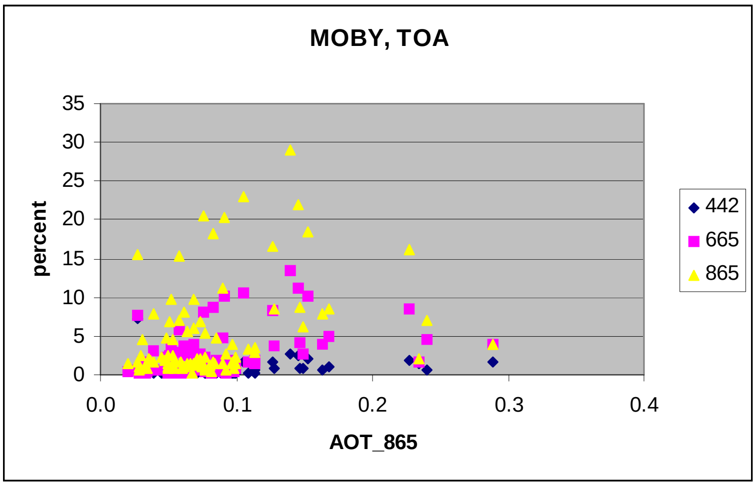

Figure 4: Relative dispersion of the MERIS TOA signal for the MOBY window depending on the AOT_865.

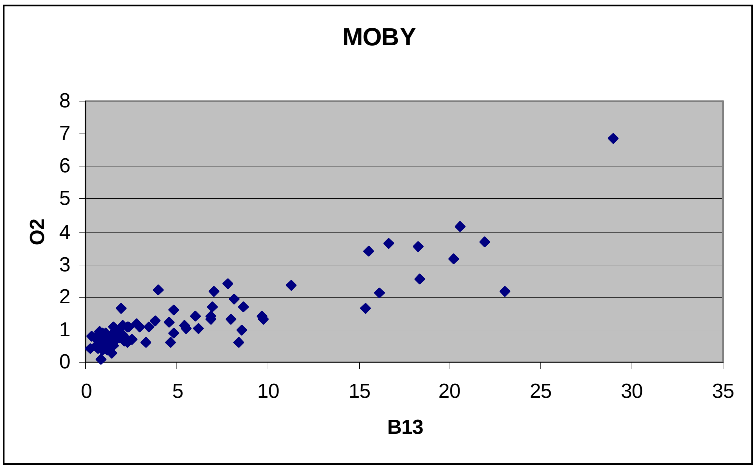

Figure 5: Relative dispersion of the MERIS TO$_2$ for the MOBY window depending on the dispersion in B13 (865 nm).

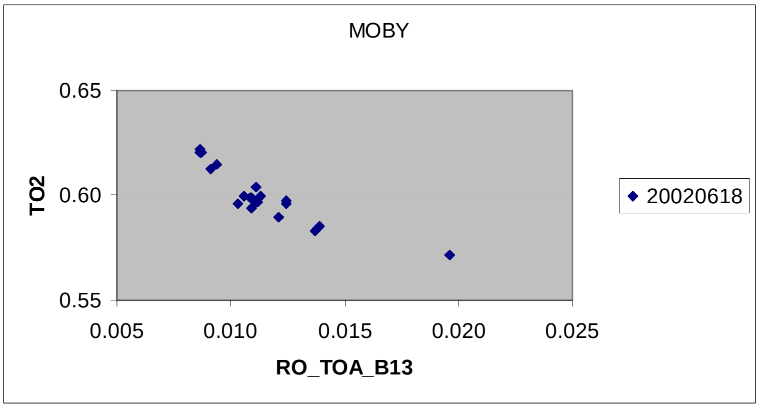

Figure 6: Relative dispersion of the MERIS TO_2 for the MOBY window depending on the dispersion in B13 (865 nm).

2.3.2 Over BOUSSOLE

When we have a larger of match up points for BOUSSOLE (Table 7), the spatial homogeneity (Figure 7 and Figure 8), appears a little less good than in MOBY with higher AOTS. The large distance from the nearest AERONET station in Villefranche sur mer makes BOUSSOLE to be used for vicarious calibration.

Table 7: spatial dispersion of MERIS TOA signal in BOUSSOLE

date	#	AOT	443	665	885	date	#	AOT	443	665	885
20030926	25	0.187	0.3	0.7	0.8	20050409	25	0.065	0.4	0.5	0.8
20031005	25	0.490	1.0	2.5	2.5	20050415	25	0.167	0.7	2.8	4.1
20031006	17	0.024	0.2	0.4	0.5	20050425	20	0.112	0.6	0.7	0.8
20031019	23	0.096	1.8	4.6	6.9	20050504	12	0.279	4.1	13.3	17.2
20031024	25	0.031	0.3	1.8	2.9	20050704	20	0.072	0.2	0.3	0.2
20031106	25	0.060	0.3	1.0	1.4	20050707	10	0.209	0.6	3.0	4.3
20031129	17	0.018	0.2	0.2	0.6	20050713	16	0.075	0.3	2.1	3.1
20040316	25	0.146	0.4	1.2	1.8	20050801	24	0.194	0.1	0.4	0.6
20040326	25	0.117	1.7	7.4	10.7	20050808	15	0.092	0.2	0.6	0.9
20040401	25	0.132	0.9	1.1	1.5	20050817	25	0.078	0.2	0.7	0.9
20040405	25	0.080	1.0	0.6	1.2	20050830	25	0.103	0.1	0.3	0.4
20040513	3	0.175	1.8	4.5	5.8	20050923	25	0.097	0.5	0.8	0.9
20040529	23	0.097	0.4	1.3	1.7	20050930	25	0.192	2.1	6.6	8.6
20040604	25	0.022	0.2	0.3	0.6	20051009	25	0.046	0.3	0.5	0.8
20040607	21	0.077	0.1	0.4	0.6	20051013	25	0.165	0.2	0.4	0.4
20040620	25	0.099	0.3	0.9	1.3	20051025	13	0.265	4.3	16.4	21.2
20040703	25	0.207	0.9	3.4	4.6	20051028	25	0.141	0.7	2.1	2.6
20040706	4	0.193	0.3	0.9	1.1	20051029	25	0.120	0.3	1.0	1.2
20040807	20	0.103	0.4	2.0	3.0	20051101	24	0.126	1.0	4.3	6.0
20040819	20	0.146	0.5	1.1	1.5	20051110	25	0.080	0.2	0.6	1.0
20040823	12	0.120	0.0	0.3	0.5	20051111	25	0.036	0.1	0.2	0.4
20040826	25	0.063	0.1	0.8	1.1	20051117	2	0.279	4.8	19.6	26.2
20040829	19	0.167	2.6	9.2	12.3	20051130	2	0.126	0.5	2.8	4.7
20040901	24	0.140	1.1	3.3	4.4	20051206	8	0.051	0.3	0.9	1.3
20040920	17	0.116	0.8	2.2	2.7	20051215	25	0.084	0.5	2.4	3.3
20040923	25	0.095	0.8	5.7	8.9	20060103	25	0.093	0.2	0.7	1.0
20040926	25	0.112	0.2	0.9	1.3	20060104	24	0.087	0.4	0.8	1.3
20040927	20	0.027	0.1	0.3	0.2	20060110	25	0.081	0.3	1.0	1.2
20041006	7	0.201	0.2	0.9	1.0	20060113	5	0.177	1.5	8.5	13.2
20041008	21	0.349	0.6	1.5	1.7	20060119	25	0.072	0.3	1.1	1.3
20041024	4	0.379	2.3	9.4	11.7	20060210	25	0.164	0.6	1.7	2.1
20041110	20	0.072	1.5	6.0	8.8	20060211	25	0.044	0.3	0.3	0.6
20041120	21	0.061	0.2	0.6	0.8	20060708	25	0.049	0.2	0.5	0.7
20041202	14	0.130	1.6	5.5	7.4	20060711	25	0.077	0.2	0.5	0.7
20041211	4	0.094	0.3	1.9	2.4	20060714	5	0.140	0.1	0.4	0.6
20041214	25	0.060	0.2	0.4	0.4	20060727	14	0.178	1.2	5.6	7.9
20050301	3	0.201	1.9	4.9	6.5	20060730	25	0.141	1.2	6.2	9.2
20050308	25	0.057	0.2	0.3	0.4	20060812	24	0.174	0.7	3.4	4.9
						20060818	25	0.089	0.3	1.9	2.3
						20060821	24	0.083	0.2	0.7	1.0
						20060831	25	0.030	0.3	0.2	0.3

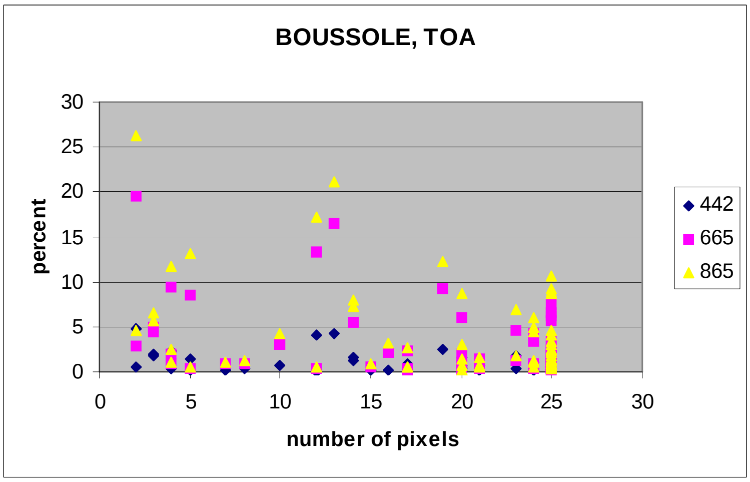

Figure 7: Same as Figure 3 but in BOUSSOLE

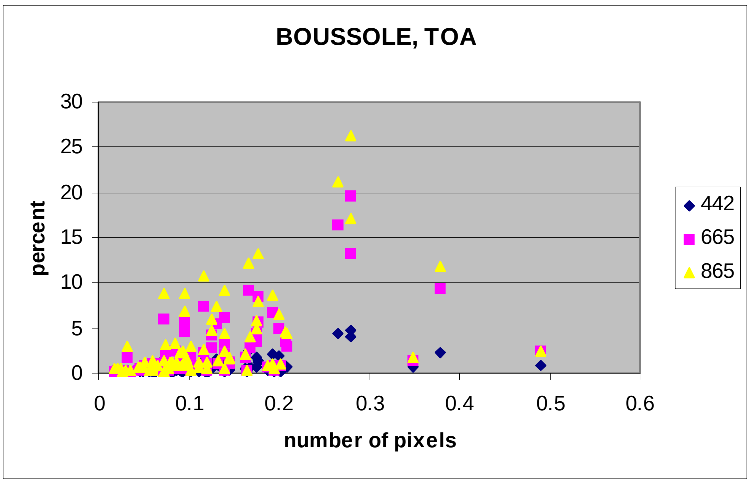

Figure 8: Same as Figure 4 but in BOUSSOLE

2.3.3 Over Venice

For Venice (Table 8), the dispersion, reported in Figure 9 and Figure 10, suggests a surprising good spatial homogeneity in the MERIS level 1 at least in the “aerosol” bands. It is surprising because in coastal areas, you expect to have different local sources of aerosols which make the complexity of the atmosphere. In the blue, there are indications of a larger spatial variability in the case 2 waters. This spatial variability of the surface should be examined mainly using level 2 product in order to emphasise the surface contribution.

As above, the use of TO_2 is a good approach for quality check of the homogeneity of the aerosols as suggests by Figure 11.

Table 8: Spatial dispersion of MERIS TOA signal in AAOT

date	#	AOT	443	665	885	O2	TH2O
20070914	25	0.159	0.44	0.66	1.11	1.34	1.25
20070709	9	0.209	0.80	0.96	1.24	1.42	1.94
20070414	20	0.197	0.21	0.44	1.16	1.71	3.32
20070323	25	0.076	0.30	0.44	0.64	0.84	1.43
20070219	18	0.100	0.29	0.50	1.07	1.33	2.41
20061103	18	0.037	0.26	0.43	0.88	1.02	1.51
20061102	10	0.073	0.52	1.02	2.08	2.66	4.56
20061011	20	0.108	0.33	0.58	1.66	2.31	3.82
20060906	18	0.127	0.49	1.08	2.99	4.31	7.34
20060423	25	0.198	0.34	0.45	0.95	1.06	1.35
20060404	25	0.032	0.25	0.57	1.31	1.84	3.23
20060302	4	0.226	0.17	0.21	0.39	0.45	0.51
20060211	25	0.024	0.28	0.49	0.74	0.77	0.97
20060111	3	0.026	0.55	0.96	1.85	2.30	3.16
20060110	25	0.035	0.56	1.22	2.60	3.16	4.79
20051118	25	0.038	0.13	0.30	0.97	1.25	1.80
20051114	22	0.229	1.06	1.31	1.96	2.27	3.02
20051111	6	0.137	0.47	0.65	0.80	0.83	1.02
20051108	4	0.100	0.18	0.15	0.18	0.32	0.51
20051013	25	0.205	0.67	1.05	1.85	2.30	3.88
20050924	25	0.096	0.32	0.60	1.25	1.50	3.20
20050912	25	0.067	0.36	0.77	1.66	2.14	3.38
20050527	13	0.106	0.72	0.89	1.08	1.16	1.54
20050422	25	0.099	0.48	0.59	0.92	1.20	1.71
20050403	25	0.125	0.37	0.60	1.22	1.36	1.65
20050307	25	0.156	0.48	0.64	0.80	0.95	1.31
20050301	25	0.160	0.73	1.27	2.64	3.68	6.83
20050210	25	0.065	0.40	0.64	1.10	1.38	1.69
20050116	25	0.050	0.23	0.25	0.41	0.55	1.10
20041215	25	0.057	0.78	1.36	2.52	3.16	4.78
20041209	25	0.109	0.53	0.87	1.75	2.18	2.97
20041120	22	0.020	0.20	0.30	0.65	0.77	0.99
20041119	2	0.219	0.01	0.01	0.01	0.01	0.01
20041116	21	0.085	3.16	3.88	5.15	5.78	7.22
20041107	19	0.048	0.30	0.56	1.23	1.50	2.05
20041016	10	0.118	2.47	3.38	5.25	6.37	9.71
20040927	20	0.027	1.54	2.79	5.32	6.62	8.85
20040905	5	0.123	0.06	0.09	0.21	0.31	0.64
20040902	21	0.089	0.14	0.25	0.58	0.85	1.65
20040823	2	0.075	0.19	0.48	1.01	1.44	2.14
20040820	7	0.200	0.43	0.73	1.63	2.48	4.71
20040722	10	0.268	0.26	0.38	0.58	0.76	1.21
20040217	4	0.139	0.12	0.11	0.20	0.36	1.36
20040103	11	0.323	0.22	0.26	0.35	0.41	0.83
20031218	24	0.077	1.07	1.59	2.49	2.76	3.58
20031208	22	0.092	0.25	0.33	0.44	0.59	1.15
20031205	20	0.223	0.75	1.15	1.88	2.00	2.03
20031129	25	0.034	0.16	0.28	0.56	0.68	0.93
20031113	25	0.146	0.30	0.47	0.98	1.23	1.85
20031110	25	0.086	0.56	1.05	1.96	2.35	3.43
20031104	25	0.078	0.43	0.85	1.82	2.16	2.43
20031010	25	0.079	0.50	0.97	2.25	2.89	4.44
20030917	25	0.096	0.58	1.08	2.39	2.98	4.12
20030914	25	0.162	0.46	0.92	2.09	2.69	3.84
20030902	25	0.080	0.20	0.37	0.89	1.33	2.54
20030501	15	0.218	0.43	0.57	0.85	0.96	1.47
20030424	8	0.225	0.83	1.09	1.48	1.76	2.34
20030418	25	0.174	0.60	0.96	2.03	2.62	4.40
20030323	25	0.128	0.22	0.28	0.41	0.63	1.87
20030314	23	0.098	0.44	0.61	0.83	0.73	0.82

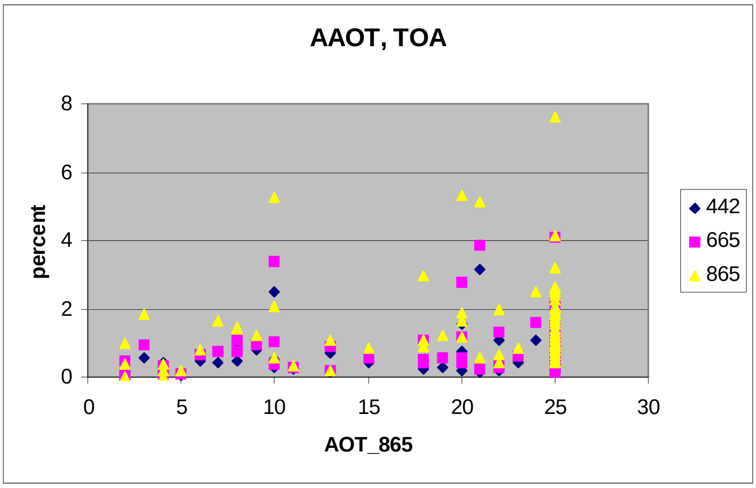

Figure 9: Same as Figure 3 but in AAOT

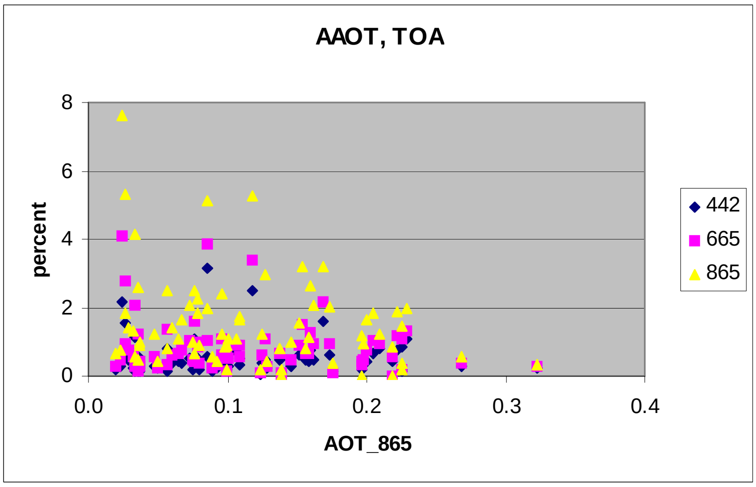

Figure 10: Same as Figure 4 but in AAOT

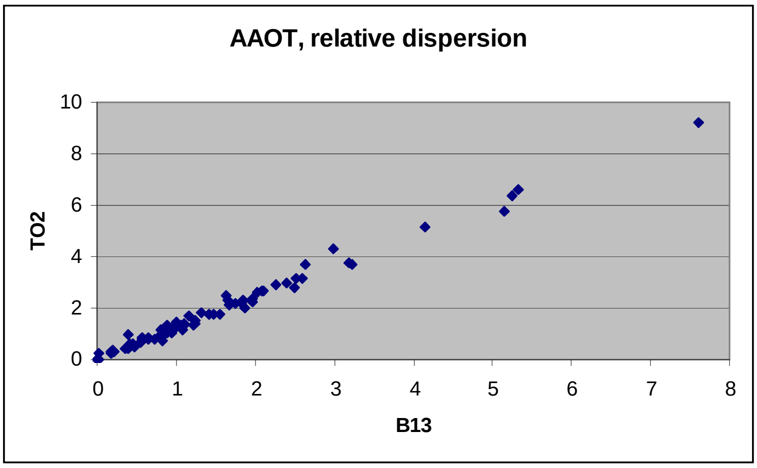

Figure 11: Relative dispersion of the MERIS TO_2 for the AAOT window depending on the dispersion in B13 (865 nm).

2.4 Conclusion

The two major Sea Equipped Sites (MOBY and BOUSSOLE) and AAOT (as representative of the AERONET OC network) have been evaluated.

BOUSSOLE, because of the lack of atmospheric measurements, appears more as a validation site than a calibration site.

MOBY and AAOT present complementarities in terms of:

- geometrical conditions,
- type of waters,
- type of atmosphere.

A recommendation of selecting one or the other sites needs to be examined after an error analysis.

The use of the O_2 band is a plus as a tool for QC.

This Page Is Intentionally Blank